New Phytologist

Selective deployment of virulence effectors correlates with host specificity in a fungal plant pathogen

Yoshihiro Inoue[1], Trinh Thi Phuong Vy[1], Suthitar Singkaravanit-Ogawa[1], Ru Zhang[1], Kohji Yamada[2], Taiki Ogawa[1], Junya Ishizuka[1], Yoshihiro Narusaka[3] and Yoshitaka Takano[1]

[1]Graduate School of Agriculture, Kyoto University, Kyoto 606-8502, Japan; [2]Graduate School of Technology, Industrial and Social Sciences, Tokushima University, Tokushima 770-8513, Japan; [3]Research Institute for Biological Sciences, Okayama Prefectural Technology Center for Agriculture, Forestry and Fisheries, Okayama 716-1241, Japan

Authors for correspondence:
Yoshitaka Takano
Email: takano.yoshitaka.2x@kyoto-u.ac.jp

Yoshihiro Inoue
Email: inoue.yoshihiro.6m@kyoto-u.ac.jp

Received: *22 November 2022*
Accepted: *27 January 2023*

New Phytologist (2023) **238:** 1578–1592
doi: 10.1111/nph.18790

Key words: *Colletotrichum orbiculare*, host specificity, phytopathogenic fungi, transcriptional control, virulence effector.

Summary

- The hemibiotrophic fungal plant pathogen *Colletotrichum orbiculare* is predicted to secrete hundreds of effector proteins when the pathogen infects cucurbit crops, such as cucumber and melon, and tobacco (*Nicotiana benthamiana*), a distantly related Solanaceae species. Here, we report the identification of sets of *C. orbiculare* effector genes that are differentially required for fungal virulence to two phylogenetically distant host species.
- Through targeted gene knockout screening of *C. orbiculare* 'core' effector candidates defined based on *in planta* gene expression, we identified: four host-specific virulence effectors (named effector proteins for cucurbit infection, or EPCs) that are required for full virulence of *C. orbiculare* to cucurbit hosts, but not to the Solanaceae host *N. benthamiana*; and five host-nonspecific virulence effectors, which collectively contribute to fungal virulence to both hosts.
- During host infection, only a small subset of genes, including the host-specific *EPC* effector genes, showed preferential expression on one of the hosts, while gene expression profiles of the majority of other genes, including the five host-nonspecific effector genes, were common to both hosts.
- This work suggests that *C. orbiculare* adopts a host-specific effector deployment strategy, in addition to general host-blind virulence mechanisms, for adaptation to cucurbit hosts.

Introduction

Plant disease disrupts food production in agricultural settings, with recurrent outbreaks of endemic and emerging microbial pathogens (Ristaino *et al.*, 2021). Although plants can be devastated by pathogens, they have a sophisticated immune system to protect themselves against the majority of microbial attacks (Schulze-Lefert & Panstruga, 2011; Panstruga & Moscou, 2020). Conversely, most fungal plant pathogens show host species specificity: specific parasitism on a limited range of host species to which they are adapted. Successful fungal plant pathogens secrete effector arsenals and deal effectively with the defense that plant species mount against nonadapted microbial intruders to establish basic compatibility with their host (Heath, 1981; Niks & Marcel, 2009; Dodds & Rathjen, 2010; Toruño *et al.*, 2016). Fungal genomes often encode suites of hundreds of diverse candidate effector genes that differ markedly among the pathogen species (Thordal-Christensen *et al.*, 2018). Despite considerable efforts to characterize effector functions over the past decade, only a small fraction of effectors have been characterized for their contribution to fungal virulence, limiting our understanding of how effectors shape the host species specificity of fungal plant pathogens.

The genus *Colletotrichum* (Sordariomycetes, Ascomycota) comprises > 190 species, which include pathogens that associate with a wide range of plant species including monocots and dicots of economic importance (O'Connell *et al.*, 2012; Jayawardena, 2016). Like many other *Colletotrichum* species, the cucumber anthracnose fungus *Colletotrichum orbiculare* has a hemibiotrophic lifestyle, with an initial symptomless biotrophic phase followed by a necrotrophic phase associated with symptoms; these phases are accompanied by waves of stage-specific gene expression (Münch *et al.*, 2008; O'Connell *et al.*, 2012; Damm *et al.*, 2013; Gan *et al.*, 2013). The pathogen develops specialized infection structures called appressoria that mediate the direct penetration of host epidermal cells, followed by the development of bulbous biotrophic hyphae within living host cells and then, at a later stage, thinner necrotrophic hyphae that kill host tissues (Perfect *et al.*, 1999; Gan *et al.*, 2013; Kubo & Takano, 2013; Irieda *et al.*, 2014).

Phylogenetically, *C. orbiculare* is closely related to pathogens of several other herbaceous hosts belonging to the Asteraceae, Fabaceae, and Malvaceae (Damm *et al.*, 2013). They show distinct host specificity at the host family level (Liu *et al.*, 2007) and constitute the *C. orbiculare* species complex (or the orbiculare clade; Cannon *et al.*, 2012; Damm *et al.*, 2013), which is

characterized by an expanded genome size relative to other *Colletotrichum* fungi from different phylogenetic groups (de Queiroz *et al.*, 2017; Gan *et al.*, 2019). In addition to cucurbit hosts such as cucumber, melon, watermelon, and wax gourd (Shivas *et al.*, 2016; Matsuo *et al.*, 2022), *C. orbiculare* is reported to infect a distantly related Solanaceae species, *Nicotiana benthamiana* (Takano *et al.*, 2006), making it a unique pathosystem in which to study the molecular basis of infection strategies toward distantly related hosts.

Like other *Colletotrichum* fungi, *C. orbiculare* is predicted to encode hundreds of effector-like small secreted proteins, which are delivered to a biotrophic interface located at appressorial penetration pores and around the primary invasion hyphae (Kleemann *et al.*, 2012; Gan *et al.*, 2013; Irieda *et al.*, 2014). Among this large repertoire of predicted effector candidates in *C. orbiculare*, only a few have been characterized. NIS1 (necrosis-inducing secreted protein 1) is an effector protein that is widely conserved among fungal pathogens and suppresses plant immunity by interacting with host BAK1 (brassinosteroid insensitive 1-associated kinase 1) and BIK1 (Botrytis-induced kinase 1) receptor-like kinases (Irieda *et al.*, 2019), besides being recognized by *N. benthamiana* and inducing cell death (Yoshino *et al.*, 2012). Despite its PTI (pattern-triggered immunity)-suppressing ability when transiently expressed in *N. benthamiana*, the NIS1 knockout (KO) mutant of *C. orbiculare* was not affected in virulence (Yoshino *et al.*, 2012), indicating that NIS1 is dispensable for host infection by *C. orbiculare*, possibly due to functional complementation by other effector protein(s). The NIS1-induced cell death in *N. benthamiana* is suppressed by an effector, CoDN3 (Yoshino *et al.*, 2012), whose calmodulin-binding ability is necessary for its function (Isozumi *et al.*, 2019). To date, CoMC69, a conserved small secreted protein of unknown function, is the only example of *C. orbiculare* effector-like proteins required for successful host infection (Saitoh *et al.*, 2012). Although these effectors were identified through *in planta* expression screening in a model system (for NIS1) or by homology to known effector proteins from other fungi (for CoDN3 and CoMC69), systematic functional screening of the effector candidates for their contribution to fungal virulence has not been performed, limiting our understanding of the genetic and molecular basis of successful infection of cucurbits and Solanaceae hosts by this pathogen.

In this study, through in-depth *in planta* transcriptome analysis of multiple *C. orbiculare* isolates, we identified 30 *C. orbiculare* 'core' effector candidates that are highly induced and expressed during the early stages of cucumber host infection. Functional screening by targeted gene KO revealed four unrelated secreted proteins of unknown function that are required for full virulence to the Cucurbitaceae host, cucumber, but not to the Solanaceae host, *N. benthamiana*. We designated them as effector proteins for cucurbit infection (EPCs) 1–4. The *EPC* KO mutants were attenuated in appressorium-mediated epidermal cell invasion and biotrophic invasive hyphal growth on cucumber, while no defect was detected for appressorium development. Quadruple KO of the four *EPCs* resulted in severe reduction or almost complete loss of virulence to cucurbit hosts but not to *N. benthamiana*, confirming the contribution of *EPCs* to cucurbit host-specific virulence. Comparative transcriptome analysis revealed higher expression of the *EPC* genes on cucumber than on *N. benthamiana*, partially explaining the cucurbit host-specific requirement of *EPCs* for fungal virulence. In addition, we identified five unrelated secreted proteins whose simultaneous deletion resulted in virulence reduction in both cucumber and *N. benthamiana*. These five genes were highly expressed during infection on both cucumber and *N. benthamiana* and represented the most highly expressed secreted protein genes of *C. orbiculare*. Our findings suggest that different sets of effector proteins are required and employed for infection of distinct hosts by *C. orbiculare* via transcriptional regulation, highlighting the host-specific infection strategy by this fungal plant pathogen through transcription-based control of essential effector genes.

Materials and Methods

Fungal strains and transformation

Colletotrichum orbiculare Damm, P.F. Cannon & Crous isolates used are listed in Supporting Information Table S1. For targeted gene disruption, the Δ*lig4* strain of 104-T (Zhang *et al.*, 2021) was used as the recipient. All fungal strains were maintained on PDA plates at 24°C in the dark. Protoplasts of *C. orbiculare* were prepared and transformed as described previously (Takano *et al.*, 2001). Hygromycin-resistant transformants were selected on PDA plates containing hygromycin B (100 μg ml^{-1}). Bialaphos-resistant transformants were selected on plates (yeast nitrogen base without amino acids (Difco; Becton, Dickinson & Co., Sparks, MD, USA), 1.6 g l^{-1}; asparagine, 2.0 g l^{-1}; NH_4NO_3, 1.0 g l^{-1}; glucose, 10 g l^{-1}; pH to 6.0 with Na_2HPO_4; agar 15 g l^{-1}) containing bialaphos (25 μg ml^{-1}). Fungal transformants were confirmed by colony PCR with primers listed in Table S2. Details of the fungal transformants generated in this study are described in Table S3. Cre/*loxP*-mediated selection marker removal was performed as described in Yamada *et al.* (2023). Briefly, conidia formed on 3-d-old cultures on PDA plates containing 2% xylose were spread on PDA plates containing 0.1 μM FdU (2′-deoxy-5-fluorouridine) for negative selection of the Cre/*loxP* cassette. Removal of the selection marker was confirmed by colony PCR and a sensitivity test on antibiotic-containing plates.

RNA isolation and sequencing

The abaxial sides of 10-d-old cucumber (*Cucumis sativus* L.) cotyledons were drop-inoculated with a conidial suspension (1×10^6 conidia ml^{-1}) of *C. orbiculare*. The inoculated plants were incubated at 24°C and harvested at 24-, 48-, and/or 72-h postinoculation (hpi). Abaxial epidermal strips were peeled, immediately frozen in liquid nitrogen, and stored at −80°C. Total RNA was extracted from the peeled strips using an Agilent Plant RNA Isolation Mini Kit (Agilent Technologies, Santa Clara, CA, USA). Three biological replicates were prepared for

each time point. Stranded RNA-seq libraries were prepared using a TruSeq Stranded mRNA LT Sample Prep Kit (Illumina, San Diego, CA, USA) and subjected to single-end sequencing with 50 cycles on the HiSeq 2000/2500 platforms.

Gene prediction and functional annotation

Gene prediction and functional annotation were performed using the FUNANNOTATE pipeline (v.0.6.0; https://github.com/nextgenusfs/funannotate). The repeat elements in the published *C. orbiculare* genome assembly (Gan *et al.*, 2019) were masked by REPEATMASKER (v.4.0.7; http://www.repeatmasker.org) using a custom repeat library constructed using REPEATMODELER (v.1.0.8; http://www.repeatmasker.org). RNA-seq reads of 104-T from different tissues/conditions (Table S4) were assembled by the genome-guided module in TRINITY (v.2.5.1; Grabherr *et al.*, 2011), and the predicted transcripts were then aligned to the softmasked genome to construct PASA (v.2.1.0; Haas *et al.*, 2003) gene models. In addition, gene models were constructed by the *ab initio* gene predictors AUGUSTUS (v.3.3; Stanke *et al.*, 2006) and GENEMARK-ET (v.4.48; Lomsadze *et al.*, 2014) with the BRAKER1 (v.1.10) pipeline (Hoff *et al.*, 2016). EVIDENCEMODELER (v.0.1.3; Haas *et al.*, 2008) then combined all *ab initio* gene model predictions, PASA gene models, and protein evidence from the UNIPROTKB/SWISS-PROT database to generate a final set of protein-coding genes. The predicted genes were functionally annotated based on BLASTP (v.2.9.0+; Altschul *et al.*, 1997) or HMMER (v.3.1b2; Eddy, 2011) searches of their protein sequences against the MEROPS (Rawlings *et al.*, 2018), PFAM (Mistry *et al.*, 2021), DBCAN (Yin *et al.*, 2012), EGGNOG (Huerta-Cepas *et al.*, 2016), and INTERPRO (Blum *et al.*, 2021) databases. Transmembrane and secreted proteins were annotated using PHOBIUS (v.1.0.1; Käll *et al.*, 2004) and SIGNALP (v.4.1; Nielsen, 2017). Default FUNANNOTATE parameters were used for all software unless otherwise specified.

Transcriptome profiling

RNA-seq reads from different tissues/conditions (Table S4) were mapped to the published *C. orbiculare* genome assembly (Gan *et al.*, 2019) using HISAT2 (Kim *et al.*, 2019). Read counts were obtained using RSUBREAD (v.1.24.2; Liao *et al.*, 2019), and transcripts per million (TPM) values (Li & Dewey, 2011) were calculated. Differential expression analysis was performed in EDGER (v.3.28.1; Robinson *et al.*, 2010) with the glmTreat function after TMM normalization (McCarthy & Smyth, 2009; Robinson & Oshlack, 2010; McCarthy *et al.*, 2012). Hierarchical clustering was performed with Ward's method and the Euclidean distance of the *Z*-scored TPM values and was represented as a heatmap using COMPLEXHEATMAP (v.2.2.0; Gu *et al.*, 2016) in RSTUDIO (v.1.2.5001).

Plasmid construction

To generate single-gene KO mutants, KO vectors were constructed by assembling *c.* 2-kb upstream and *c.* 2-kb downstream fragments of the target gene, a hygromycin or bialaphos resistance gene cassette, and a vector backbone generated by digestion of pCB1636 (Sweigard *et al.*, 1997) with *Xho*I and *Hin*dIII via In-Fusion cloning (TaKaRa Bio, Otsu, Japan). To generate multigene KO mutants, KO vectors were constructed by assembling a fragment generated by PCR fusion of *c.* 2-kb upstream and *c.* 2-kb downstream fragments of the target gene and a Cre/*loxP* cassette containing the hygromycin or bialaphos resistance gene and a vector backbone generated by digestion of pCB1636 with *Xho*I and *Hin*dIII via In-Fusion cloning. To construct CRISPR/Cas9 expression vectors targeting effector candidates, sense and antisense oligonucleotides were annealed and ligated with pChPtef026 (Yamada *et al.*, 2023) digested with *Bsa*I. To construct complementation vectors, a genomic fragment containing *c.* 2-kb upstream, coding, and *c.* 1-kb downstream sequences, a Cre/*loxP* cassette containing the hygromycin resistance gene, and a vector backbone generated by digestion of pCB1636 with *Xho*I and *Hin*dIII were assembled via In-Fusion cloning. Genomic fragments were PCR-amplified from genomic DNA of *C. orbiculare* 104-T with primers listed in Table S2. The hygromycin resistance gene cassette was PCR-amplified from pCB1636 with primers Hyg_F and Hyg_R. The bialaphos resistance gene cassette was PCR-amplified from pCB1636BAR with primers Bar_F and Bar_R. The Cre/*loxP* cassette containing the hygromycin or bialaphos resistance gene was PCR-amplified from pCB1636 pks1 clox HPT-TK vector or pCB1636 pks1 clox Bar-TK vector (Yamada *et al.*, 2023), respectively, with primers clox_F and clox_R. Details of plasmid construction are described in Table S5.

Virulence assays

Conidial suspensions (5×10^5 conidia ml^{-1}) collected from 7-d-old PDA cultures were used for drop inoculation of detached cotyledons from 10-d-old plants (cucumber cv Suyo or melon (*Cucumis melo* L.) cv Lennon) or leaves from 5 to 6-wk-old *N. benthamiana* Domin plants. For assessment of virulence phenotype, the lesions developed were scored after incubation for 7 d at 24°C. To allow paired comparisons to be made on the same leaf, we inoculated one half of the leaf with the parental strain (104-TΔ*lig4*) and the other half with a mutant strain of interest. For each leaf, the area of the lesion formed was measured for each of the strains using IMAGEJ (https://imagej.nih.gov/ij/). Only necrotic lesions, and not the yellowing areas, were measured. For virulence assays on cucumber and melon, lesion area data from a total of nine leaves from three independent experiments (three leaves per experiment) were obtained. Lesion areas in the recipient strain and the mutant were measured and tested for a significant difference in mean lesion area by paired *t*-test. For virulence assays on *N. benthamiana*, lesion area data from a total of three leaves from three independent experiments (one leaf per experiment) were obtained. Lesion areas from a total of 24 to 30 inoculated spots were measured per strain and normalized by subtracting the mean lesion area of the parental strain. The statistical significance of the difference in the mean lesion area was tested by Welch's *t*-test.

Microscopic observation

Conidial suspensions (5×10^5 conidia ml^{-1}) were spotted onto the abaxial sides of cotyledons of cucumber cv Suyo. The inoculated plants were incubated at 24°C for 24, 48, 72, and 96 h. The epidermal layers of cotyledons were then peeled away and mounted in water under coverslips. Appressorium formation was assessed at 24 hpi by scoring at least 100 conidia per replication. Appressorium-mediated host penetration and invasive hyphal growth were assessed at 72 and 96 hpi by scoring at least 150 appressorium-forming conidia per replication. The observed invasive hyphae (IH) were classified into three categories based on the length and degree of expansion within the host epidermal cells: Class I, IH shorter than 10 µm; Class II, IH longer than 10 µm and restricted to within the first-invaded cell; Class III, IH longer than 10 µm and extending to more than a single cell. Data from a total of nine replicates from three independent experiments (three replicates per experiment) were obtained.

Results

Expression profiling reveals *in planta*-induced 'core' secreted protein genes of *C. orbiculare*

To identify virulence effectors of *C. orbiculare* that are involved in establishing biotrophic interaction with its host, we first undertook gene expression profiling of *C. orbiculare* during the early biotrophic stages of cucumber infection. Based on cytological observation of the infection process of *C. orbiculare* strain 104-T on cucumber, we obtained *in planta* RNA-seq data at 24-, 48-, and 72-hpi of cucumber, which correspond to the (pre)penetration (24 hpi), early biotrophy (48 hpi), and established biotrophy (72 hpi) stages, respectively (Fig. S1; Table S4). To ensure that no *in planta*-expressed genes were missed, we then re-annotated the 104-T reference genome (Gan *et al.*, 2019) using the *in planta* RNA-seq dataset from infected cucumber tissues obtained in this study and an RNA-seq dataset obtained from vegetative hyphae (VH), conidia (Con), and infected *N. benthamiana* tissues at 24, 72, and 168 hpi (Gan *et al.*, 2019). As a result, we obtained 13 287 protein-coding genes (Dataset S1) and used this set for subsequent transcriptome analysis.

To identify effector candidates showing biotrophy-associated expression, we looked for differentially expressed genes (DEGs) between the *in vitro* (VH and Con) and *in planta* (24, 48, and 72 hpi of cucumber) conditions with three replicates using EDGER (glmTreat test for $|\log_2 FC| > 1$; FDR < 0.01; Fig. S2a,b). We found 177 putative secreted protein (containing an N-terminal signal peptide) genes that were both upregulated more than eightfold in any *in planta* conditions compared with the two *in vitro* conditions and highly expressed (TPM > 100 at the highest expression condition), representing *in planta*-induced highly expressed effector candidates (Fig. S2c). Hierarchical clustering of these candidates based on *Z*-scored TPM values revealed six major clusters (Fig. 1a). Cluster 2 genes showed specific induction at 72 hpi and were highly enriched with carbohydrate-active enzyme (CAZyme) genes, while members of cluster 3 with specific induction at 24 hpi rarely had functional annotation (Fig. 1c), one of the characteristics of fungal plant pathogen effectors (Kanja & Hammond-Kosack, 2020). Based on these observations, we decided to prioritize the effector candidates with high expression at 24 hpi for functional characterization.

To further refine the list of effector candidates, we additionally obtained RNA-seq data for another four *C. orbiculare* wild isolates at 24 hpi of cucumber (Tables S1, S4). We reasoned that if an effector gene is important and necessary for virulence of *C. orbiculare* to cucumber, it should be maintained and expressed in different isolates of the species. By selecting genes that are commonly highly expressed (TPM > 100) across five *C. orbiculare* isolates, we obtained a list of 30 effector candidates that constitute the *in planta*-induced 'core' secreted protein genes of *C. orbiculare* (Figs 1, 2a; Table S6).

Four unrelated secreted proteins are specifically required for full virulence to a cucurbit host, cucumber but not to a Solanaceae host, *N. benthamiana*

To assess the contribution of the effector candidates to fungal virulence, we generated targeted gene KO mutants of individual candidates. To facilitate the targeted gene KO through homologous recombination, we deployed a *Ligase4* KO mutant of 104-T (Δ*lig4*) (Zhang *et al.*, 2021) as a recipient strain that is reduced in the ability of nonhomologous end joining, with the aid of a targeted double-strand break induced by the Cas9 nuclease (Yamada *et al.*, 2023). As a result, we successfully generated KO mutants for 27 of the 30 effector candidates (Fig. 2; Table S6).

To quantify the virulence effect of these KO mutants, we inoculated cucumber cotyledons with KO mutants and measured the lesion size formed by infection. To allow paired comparisons to be made on the same leaf, we inoculated one half of the cotyledon with the parental strain (Δ*lig4* mutant) and the other half with a KO mutant (Fig. S3). Initially, we arbitrarily picked one KO mutant from each of the effector candidates and measured the virulence effect (Fig. 2b); we observed a significant (paired *t*-test; $P < 0.05$) reduction of lesion size in the KO mutant for four effector candidates, namely g_04238, g_04157, g_10510, and g_11868 (Fig. 2b). The virulence reduction was consistent in two independent KO mutants, and the KO mutant phenotypes were complemented by the introduction of genomic fragments containing the respective genes (Fig. 2c,d), indicating that the four genes are virulence factors of *C. orbiculare* and required for full virulence to cucumber.

In addition to cucurbit hosts, *C. orbiculare* isolate 104-T is reported to infect the Solanaceae species *N. benthamiana* (Takano *et al.*, 2006). Since the interaction between *C. orbiculare* and *N. benthamiana* is not yet well characterized, we first checked whether *C. orbiculare* isolates are generally virulent to *N. benthamiana*. All the tested *C. orbiculare* isolates ($n = 5$) were virulent on *N. benthamiana* (Fig. S4), demonstrating that the infection of *N. benthamiana* by *C. orbiculare* is not specific to the isolate 104-T. Next, we monitored and compared the disease development by *C. orbiculare* on cucurbit hosts, cucumber and melon, and *N. benthamiana*. The timing of lesion formation and development on *N. benthamiana* was similar to that on cucurbit

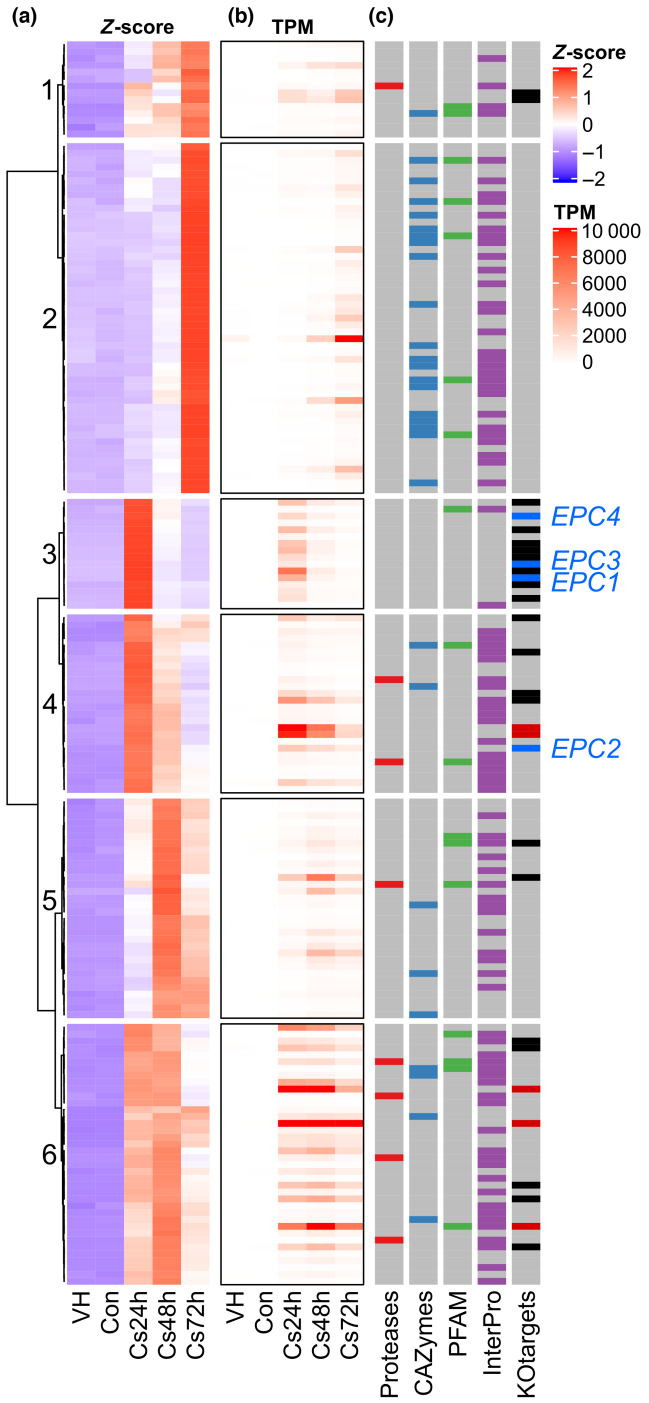

Fig. 1 Transcription profiles of 177 *in planta*-induced and highly expressed effector candidates in *Colletotrichum orbiculare* isolate 104-T. (a) Heatmap showing the expression patterns (*Z*-score of expression values) and (b) expression levels (tags per million, TPM) of the effector candidates in different conditions. (c) Gene function and category annotations. For the left four columns, genes with functional annotation in the respective category are indicated by red (proteases), blue (CAZymes), green (PFAM domains), and purple (InterPro domains) colored tiles. The rightmost column shows 30 effector candidates that represent the *in planta*-induced 'core' secreted protein genes of *C. orbiculare* and were subjected to targeted gene KO experiments. Four EPCs, the Top5 highest expression genes, and the other effector candidates are indicated in blue, red, and black, respectively. VH, vegetative hyphae; Con, conidia; Cs24h, Cs48h, Cs72h, 24, 48, 72 h after inoculation of cucumber, respectively.

hosts (Fig. S5). Third, we performed microscopic observations of the infection process of *C. orbiculare* on *N. benthamiana*. This revealed that *C. orbiculare* develops bulbous invasion hyphae (characteristic of biotrophic hyphae) from appressoria formed on *N. benthamiana* with a similar timing as on cucumber (Figs S1, S6). These data indicate that *C. orbiculare* has the ability to infect *N. benthamiana* in a similar way as it infects cucurbit hosts.

To see whether the four genes identified above are also required for full virulence to a host species from a different family, we inoculated *N. benthamiana* with the effector KO mutants and measured the virulence effect. In contrast to the results on cucumber, no significant virulence reduction was detected for any of the four effector candidates on *N. benthamiana* (Fig. 2e,f), suggesting that the four effector candidates are required for full virulence on the Cucurbitaceae host cucumber but not on the Solanaceae host *N. benthamiana*. We therefore named these candidates effector proteins for cucurbit infection (EPCs) 1–4.

The four EPCs' sequences were unrelated (Figs S7–S10) and had no Pfam or InterProScan hits (Fig. 1). *EPC1* (g_04238), encoding a secreted protein of 195 amino acids (aa), showed patchy distribution among fungal plant pathogens, with homologs in *C. orbiculare* and its closely related *Colletotrichum* species belonging to the *C. orbiculare* species complex (COSC; Damm *et al.*, 2013), some forma speciales of *Fusarium oxysporum*, and distantly related Dothideomycetes fungi, *Pyrenophora* spp. (Fig. S7). *EPC1* homologs appear to have expanded specifically in the lineage of COSC, with three copies in *C. orbiculare* and two to four copies in other COSC species (Fig. S7b). Among the three homologs in *C. orbiculare*, only *EPC1* showed active transcription, and the other two homologs were barely expressed in any of the conditions tested (Fig. S7c). Despite the diversification of protein sequences among the *EPC1* homologs, six cysteine residues were highly conserved (Fig. S7d). *EPC2* (g_10510), encoding a secreted protein of 330 aa, was detected in several *Colletotrichum* species, but not outside this genus, suggesting that it is a *Colletotrichum*-specific protein (Fig. S8). *EPC2* homologs in the COSC lineage were distinguished from those of other *Colletotrichum* species by indels in the middle part of the protein (Fig. S8b). *EPC4* (g_04157), encoding a secreted glycine-rich (47.5%) protein of 514 aa, was specifically present in *Colletotrichum* species belonging to the COSC, implying that *EPC4* is a lineage-specific protein unique to the COSC (Fig. S9).

EPC3 (g_11868) encodes a secreted protein of 223 aa and shows homology to *F. oxysporum* SIX6 effector proteins (Fig. S10). Like *EPC1*, multiple copies of *EPC3* homologs were present in COSC, comprising three distinct clades (Fig. S10b). Among the three copies present in *C. orbiculare*, *EPC3* and *g_04482* showed similar expression patterns (Fig. S10c) and were included in our candidate effector list (Table S6), while the other homolog (*g_09475*) was barely expressed in any of the conditions tested (Fig. S10c). Despite *g_04482* being highly expressed *in planta*, its KO did not result in virulence reduction (Fig. 2b). Furthermore, double KO mutants of *EPC3* and *g_04482* did not show any virulence reduction compared with the *EPC3* single-gene KO mutant (Fig. S10d,e), indicating functional diversification among the members of the expanded effector family.

EPCs contribute additively to host invasion, *in planta* biotrophic growth, and virulence to cucurbits

Single-gene KO of each *EPC* gene resulted in a reduction, but not a complete loss, of virulence to cucumber (Fig. 2c,d). We then asked what would happen if we knocked out multiple *EPC* genes simultaneously. To check the collective contribution of four EPCs on fungal virulence, we generated multigene KO mutants of *EPC* genes using the self-excision Cre/*loxP* system that we recently established for *C. orbiculare* (Yamada *et al.*, 2023; Fig. S11). Double KO mutants of *EPC1* and *EPC2* (Δ*EPC1* Δ*EPC2*) showed a greater reduction of virulence (Fig. 3a,b) compared with the respective single KO mutants (Fig. 2c,d), suggesting an additive contribution of the two *EPC*s to cucumber infection. Further virulence reduction was observed for triple (Δ*EPC1* Δ*EPC2* Δ*EPC3*) and quadruple (Δ*EPC1* Δ*EPC2* Δ*EPC3* Δ*EPC4*) KO mutants (Fig. 3a–d). The observed reduction in lesion formation was correlated with a reduction of fungal biomass, and thus a reduced level of plant colonization (Fig. S12). In addition to cucumber, virulence reduction of the *EPC* KO mutants was observed in melon, another cucurbit host of *C. orbiculare* (Fig. 3c,d). Surprisingly, despite the severe or almost complete loss of virulence to the two cucurbit hosts (Fig. 3a,c), we observed no reduction of virulence to *N. benthamiana* even in the quadruple KO mutant (Fig. 3e,f). Again, this strongly suggests that EPCs are host-specific virulence factors of *C. orbiculare* that are required specifically for cucurbit host infection.

To understand which stages of infection are affected in *EPC* KO mutants, we examined the infection-related behavior of *EPC* single and multiple KO mutants following inoculation of cucumber cotyledons. Although the KO mutants showed normal appressorium formation (Fig. S13) and retained their ability to penetrate inert cellophane membranes (Fig. S14), the frequency of appressorium-mediated host invasion (invasion ratio) was lower in KO mutants compared with the parental strain, except for the Δ*EPC4* strain, which showed an invasion ratio similar to the parental strain at 3-d postinoculation (dpi; Fig. 4a). Consistent with the additive effect on fungal virulence, the invasion ratio at 4 dpi was lower in multigene KO mutants than in the respective single-gene KO mutants (Fig. 4a). However, even in the quadruple KO mutant, host invasion was not completely abolished and occurred in 15–20% of the appressoria (Fig. 4a), suggesting that other effectors contribute to the host invasion stage.

Next, to estimate the effect of *EPC* KO on biotrophic growth of invasive hyphae (IH), for each observed IH we scored the length and degree of expansion within host epidermal cells and classified them into three categories (classes I–III; Fig. 4c). In the *EPC1*, *EPC2*, and *EPC3* single-gene KO mutants, the ratio of short IH (class I) slightly increased, and long and extending IH (class III) decreased (Fig. 4c). The *EPC4* KO mutant was unique in that the ratio of longer IH classes (II and III) was dramatically reduced and *c.* 85% of the IH remained short (class I) even at 4 dpi (Fig. 4b). In *EPC* double (Δ*EPC1* Δ*EPC2*) and triple (Δ*EPC1* Δ*EPC2* Δ*EPC3*) KO mutants, the ratio of longer IH classes (II and III) gradually decreased, and in the quadruple KO (Δ*EPC1* Δ*EPC2* Δ*EPC3* Δ*EPC4*) mutant, we rarely observed longer IH (Fig. 4b) even at 4 dpi. These results suggest that EPCs additively contribute to both host invasion and subsequent intracellular biotrophic growth with different magnitudes of effect.

Gene expression patterns of *EPC*s correlate with their different contributions to virulence in cucurbits and *N. benthamiana*

We next asked why *EPC*s were specifically required for full virulence to cucurbit hosts but not to *N. benthamiana*. As an initial step to address this question, we compared the gene expression levels of the four *EPC*s using RNA-seq data from 24 hpi of cucumber and *N. benthamiana* (Table S4; Gan *et al.*, 2019). Although *EPC*s were among the top 100 highest expression genes on cucumber, they were not as highly expressed or ranked on *N. benthamiana* (Fig. 5a). In particular, the gene expression levels of *EPC1* and *EPC3* were over 20-fold lower on *N. benthamiana* than on cucumber. To validate the cucumber-specific induction of *EPC* genes observed in the RNA-seq data at 24 hpi, we performed RT-qPCR analysis at 16, 24, and 32 hpi of cucumber, melon, and *N. benthamiana*. This revealed a highly specific induction of three of the *EPC* genes (*EPC1*, *EPC3*, and *EPC4*) on cucurbit hosts across three time points, and less so for *EPC2* (Fig. 5b), confirming the observation from the RNA-seq data. In contrast to the *EPC* genes, the overall transcriptome profiles were similar between the two host species and only a small number of DEGs (241 genes; *c.* 1.8% of the whole gene sets) were detected (Fig. S15; Tables S7, S8). These DEGs with preferential expression on one of the host species were enriched for putative secreted protein genes compared with whole gene sets (Fisher's exact test; $P = 6.5e\text{-}07$). In addition, 10 of the 30 *C. orbiculare* core effector candidates defined in this study were included in the cucumber-specific DEG set (Table S7), suggesting that *C. orbiculare* employs host-specific transcriptional control of effector-like genes such as *EPC1* and *EPC3*.

Most highly expressed 'host-blind' secreted protein genes contribute to virulence in both cucumber and *N. benthamiana*

Based on the observation that the *EPC1* genes showed a host (cucurbit)-specific virulence effect with host-preferential gene expression, we hypothesized that effector candidates with 'host-blind' gene expression may include virulence factors for infection of both cucurbits and *N. benthamiana*. To test this hypothesis, we picked five effector candidate genes (hereafter, the 'Top5' genes), which represented the most highly expressed secreted protein genes both on cucumber and on *N. benthamiana* (Figs 1, 5; Table S6). Since we did not observe virulence reduction in single-gene KO mutants of the Top5 genes (Fig. 2b), we decided to generate multigene KO mutants to evaluate the potential virulence contribution of the Top5 genes (Fig. S16). Although virulence reduction was not observed in double (Δ*g_13573* Δ*g_01222*), triple (Δ*g_13573* Δ*g_01222* Δ*g_01264*), and quadruple (Δ*g_13573* Δ*g_01222* Δ*g_01264* Δ*g_09665*) KO mutants, we observed a

New Phytologist

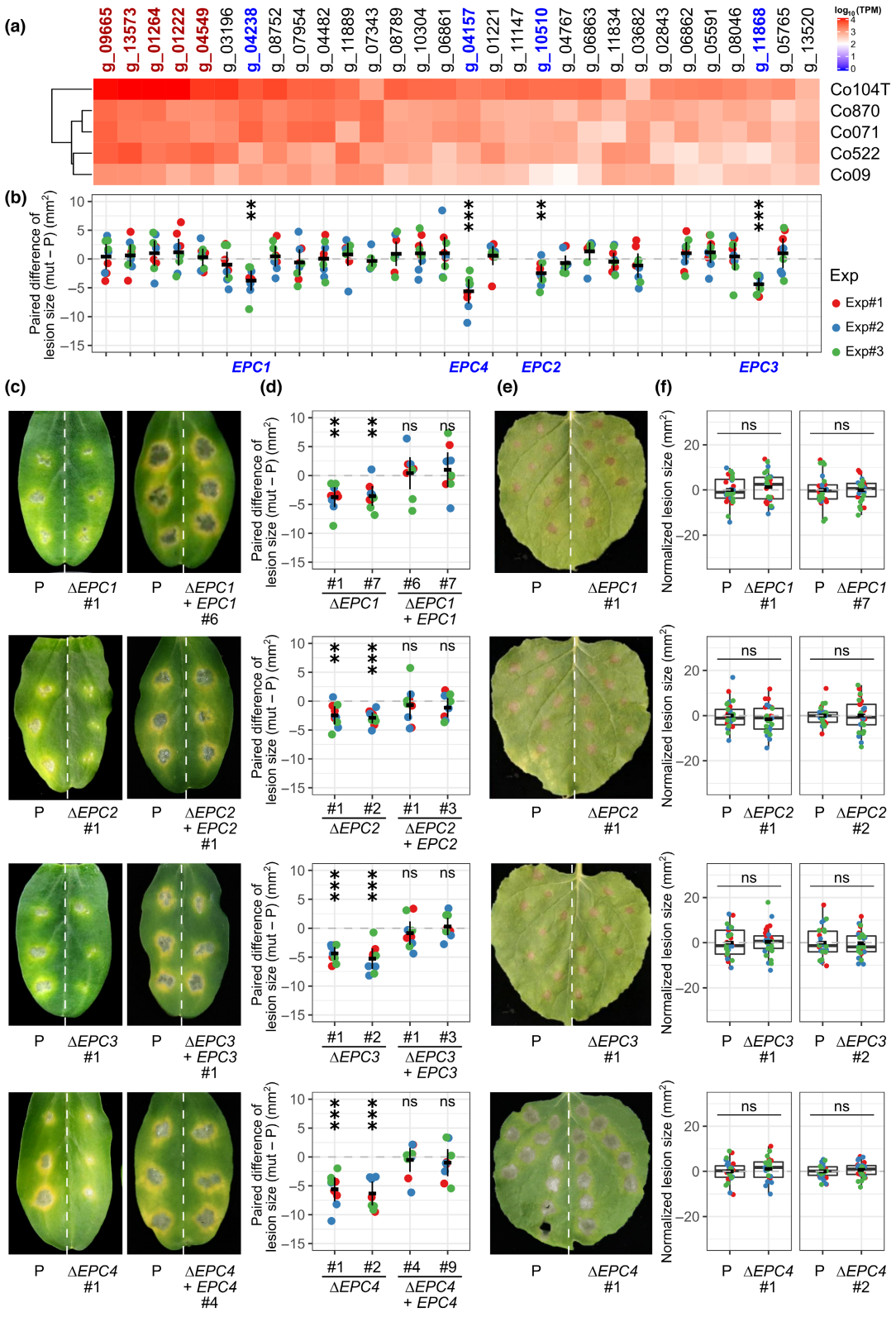

significant reduction of virulence in the quintuple (Δ*g_13573* Δ*g_01222* Δ*g_01264* Δ*g_09665* Δ*g_04549*) KO mutant, where all the Top5 genes were deleted (Fig. 6). Reintroduction of *g_04549* into the quintuple KO mutant complemented the virulence phenotype on cucumber (Fig. S17). Consistent with the host-blind transcript abundance on both hosts, and in contrast to *EPC* KO mutants, virulence reduction was observed in both cucumber and *N. benthamiana* (Fig. 6), suggesting that the Top5 genes encode virulence factors, probably with functional redundancy or relatively small individual contributions to virulence, that

Fig. 2 Targeted gene KO of *in planta*-induced core secreted protein genes of *Colletotrichum orbiculare*. (a) Heatmap showing the gene expression levels (log_{10}TPM values) of 30 effector candidates in five *C. orbiculare* isolates at 24-h postinoculation (hpi) of cucumber. Genes (on *x*-axis) are arranged in descending order based on the mean TPM values from five isolates. Names of the top 5 highest expression (Top5) genes are in red. (b) Plot showing the virulence effect (paired difference of lesion size) for KO mutants of the effector candidates in (a). For each mutant, data from nine biological replicates (nine cucumber cotyledons) from three independent experiments (three replicates from each experiment) were obtained and are represented as dots. Black horizontal bars indicate paired mean difference of lesion size between an effector KO mutant (mut) and its parent strain (104-TΔ*lig4*, P), and the associated error bars indicate the 95% confidence interval of the paired mean difference. Names of genes whose KO mutant showed a statistically significant ($P < 0.05$; paired *t*-test, $n = 9$) reduction of lesion size are in blue in (a). (c) Lesion formation by *EPC* KO mutants and their complementing strains on cucumber cotyledons. The left half of each leaf was inoculated with the parental strain for KO and the right half with test strains. Representative pictures were taken at 7-d postinoculation (dpi). (d) Plots showing the paired difference of lesion size for KO mutants and complementing strains compared with the parental strain. Data for KO mutant strains Δ*EPC1*#1, Δ*EPC2*#1, Δ*EPC3*#1, and Δ*EPC4*#2 are the same as plotted in (b). Statistical significance in the difference of the means was tested with the paired *t*-test. (e) Lesion formation by *EPC* KO mutants on *Nicotiana benthamiana* leaves. The left half of each leaf was inoculated with the parental strain for KO and the right half with KO mutant strains. Representative pictures were taken at 7 dpi. (f) Plots showing the lesion size of the parental strain and KO mutants from paired infection assays as in (e). For each leaf, lesion size data were normalized by mean lesion size of the parental strain. Lesion size data from 8 to 10 drop inoculation sites were collected for each fungal genotype per leaf. Data from 24 to 30 drop inoculation sites from three independent experiments (8–10 drop inoculation sites from one leaf per experiment) were collected. Thick horizontal bars in black indicate the mean. Center lines show the medians; box limits indicate the 25th and 75th percentiles; whiskers extend to 1.5 times the interquartile range from the 25th and 75th percentiles. Statistical significance in the difference of the means was tested with Welch's *t*-test. **, $P < 0.01$; ***, $P < 0.001$; ns, not significant ($P > 0.05$).

are necessary for general fungal virulence. The reduced virulence was attributed to the reduced level of host invasion (Fig. S18) and was not due to a reduced level of invasive hyphal growth (Fig. S18) or to developmental defects (Figs S19, S20).

Among the Top5 genes, only g_04549 had PFAM/INTERPRO hits (PF11327/IPR021476: egh16-like virulence factor; Fig. S21); it is a homolog of the appressorium-specific protein GAS1 of the rice blast fungus (Xue *et al.*, 2002). This protein is widely conserved among ascomycete and basidiomycete fungi (Valette *et al.*, 2021) and is required for host penetration in plant and insect pathogens (Huang *et al.*, 2019). The other four of the Top5 genes encoded proteins of unknown function (Table S6), which are distributed in COSC (g_09965 and g_13573; Figs S22, S23), in Sordariomycetes plant pathogens (g_01264; Fig. S24), or among diverse plant pathogenic ascomycete fungi (g_01222; Fig. S25). The observation that *g_04549* KO in the quadruple KO background, but not in the parental strain, resulted in reduced fungal virulence suggests functional redundancy among, or additive effects of different virulence functions by, a highly conserved fungal virulence factor (g_04549) and other previously uncharacterized protein(s) encoded by the Top5 genes, revealing novel fungal virulence factor(s) that were not identified without the multigene KO approach.

Discussion

In this study, we report KO-based functional screening of 27 candidate effector genes of *C. orbiculare*. These genes encode predicted secreted proteins that are conserved among five independent isolates of *C. orbiculare* (Fig. 2a) and showed *in planta*-specific expression at levels that are highest during the early stages of infection (Fig. 1). We have identified four presumptive secreted proteins (EPC1–4) of *C. orbiculare* that are specifically required for infection of Cucurbitaceae hosts but not of the Solanaceae host *N. benthamiana*. Single-gene KO for the four *EPC* genes resulted in reduced lesion formation on cucumber but not on *N. benthamiana* (Fig. 2c,d). Consistent with the specific gene expression during host invasion and early biotrophic stages of infection (Figs 1, S1), the *EPC* KO mutants showed reductions in successful host invasion and biotrophic growth inside the host cells of cucumber cotyledons, while the formation of the infection structure for host invasion (the appressorium) was unaffected (Figs 4, S13, S14). Multigene KO of all four *EPC*s resulted in the severe reduction or almost complete loss of lesion formation on cucumber and melon, but no detectable virulence defect on *N. benthamiana* (Fig. 3). Taking these observations together, we regard the EPC proteins identified here as 'host-specific' virulence effectors of *C. orbiculare* for cucurbit infection; that is, our findings provide direct evidence that virulence effectors contribute to the host species specificity of fungal pathogens. Consistent with this, recent studies in phytopathogenic *F. oxysporum* reveal, through horizontal chromosome transfer experiments, that conditionally dispensable chromosomes harboring several *SIX* effector genes are responsible for differences in host range (Li *et al.*, 2020; Ayukawa *et al.*, 2021).

*EPC*s encode unrelated secreted proteins of unknown function that differ considerably in size: EPC1, 195 aa; EPC2, 330 aa; EPC3, 223 aa; and EPC4, 514 aa. All four EPC proteins have homologs in other members of the *C. orbiculare* species complex (COSC) that have different host specificities (Figs S7–S10). This raises the possibility that EPCs confer virulence against not only cucurbits but also other plants. Sequence similarity searches revealed that three EPCs (EPC1, EPC2, and EPC4) are novel fungal virulence proteins with no resemblance to previously reported virulence factors (Table S6), while EPC3 is an ortholog of SIX6 effector proteins of the soil-borne fungal plant pathogen *F. oxysporum*. In cucurbit-infecting pathotypes such as *F. oxysporum* f. sp. *radicis-cucumerinum* and f. sp. *niveum*, the *SIX6* gene is reportedly involved in virulence on cucurbit hosts (Niu *et al.*, 2016; van Dam *et al.*, 2017), suggesting that SIX6 is an important virulence factor of fungal plant pathogens for cucurbit infection, irrespective of the infection strategy employed (root infection vs aboveground infection). In addition, SIX6 in *F. oxysporum* f. sp. *lycopersici* is required for full virulence to tomato (Gawehns *et al.*, 2014), suggesting a virulence function for SIX6 on both Cucurbitaceae and Solanaceae hosts.

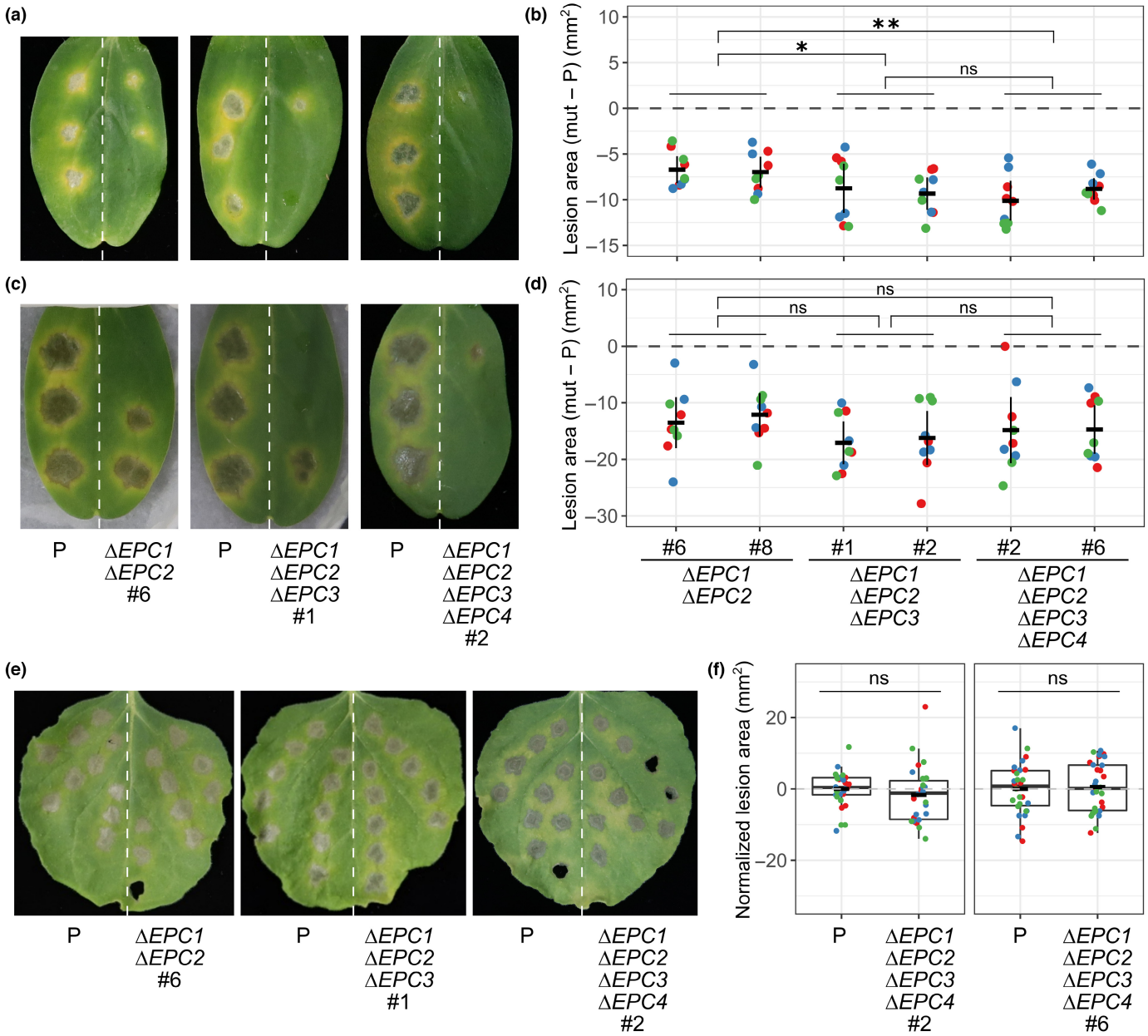

Fig. 3 Multigene KO mutants of *EPC*s are severely affected in virulence to cucumber but not to *Nicotiana benthamiana*. (a, c) Lesion formation by *EPC* multigene KO mutants on cucumber (a) and melon (c) cotyledons. The left half of the leaf was inoculated with the parental strain for KO (104-TΔ*lig4*, P) and the right half with test strains. Representative pictures taken at 7-d postinoculation (dpi) are shown. (b, d) Plots showing the virulence effect (paired difference of lesion size) for KO mutants compared with 104-TΔ*lig4* (P) on cucumber (b) and melon (d). For each mutant, data from nine biological replicates (nine cucumber cotyledons) from three independent experiments (three replicates from each experiment) were obtained and represented as dots. Thick horizontal bars in black indicate paired mean difference of lesion size between respective KO mutant (mut) and 104-TΔ*lig4* (P). Error bars indicate the 95% confidence interval of the paired mean difference. On each plant species, statistical significance in the difference of the mean among the genotypes was tested with Welch's *t*-test with Holm's multiple correction. (e) Lesion formation by *EPC* multigene KO mutants on *N. benthamiana* leaves. The left half of the leaf was inoculated with the parental strain for KO (104-TΔ*lig4*, P) and the right half with KO mutant strains. Representative pictures taken at 7 dpi are shown. (f) Boxplots showing the lesion size of 104-TΔ*lig4* (P) and KO mutants from paired infection assay as in (e). For each leaf, lesion size data were normalized by mean lesion size of the parental strain. Lesion size data from 8 to 10 drop inoculation sites were collected for each fungal genotype per leaf. Data from 24 to 30 drop inoculation sites from three independent experiments (8–10 drop inoculation sites from one leaf per experiment) were collected. Center lines show the medians; box limits indicate the 25th and 75th percentiles; whiskers extend to 1.5 times the interquartile range from the 25th and 75th percentiles. Statistical significance in the difference of the mean was tested with Welch's *t*-test. *, $P < 0.05$; **, $P < 0.01$; ns, not significant ($P > 0.05$).

Nevertheless, EPC3, a SIX6 ortholog in *C. orbiculare*, contributed specifically to cucurbit host infection but not to *N. benthamiana* infection (Fig. 2). The apparent discrepancy may be explained by cucumber host-specific expression of *EPC3* (Fig. 5); therefore, *C. orbiculare* appears to depend on and deploy EPC3 only during the infection of cucurbit hosts.

In addition to host-specific virulence factors (the *EPC* genes), our work revealed a set of secreted protein genes (the Top5 genes)

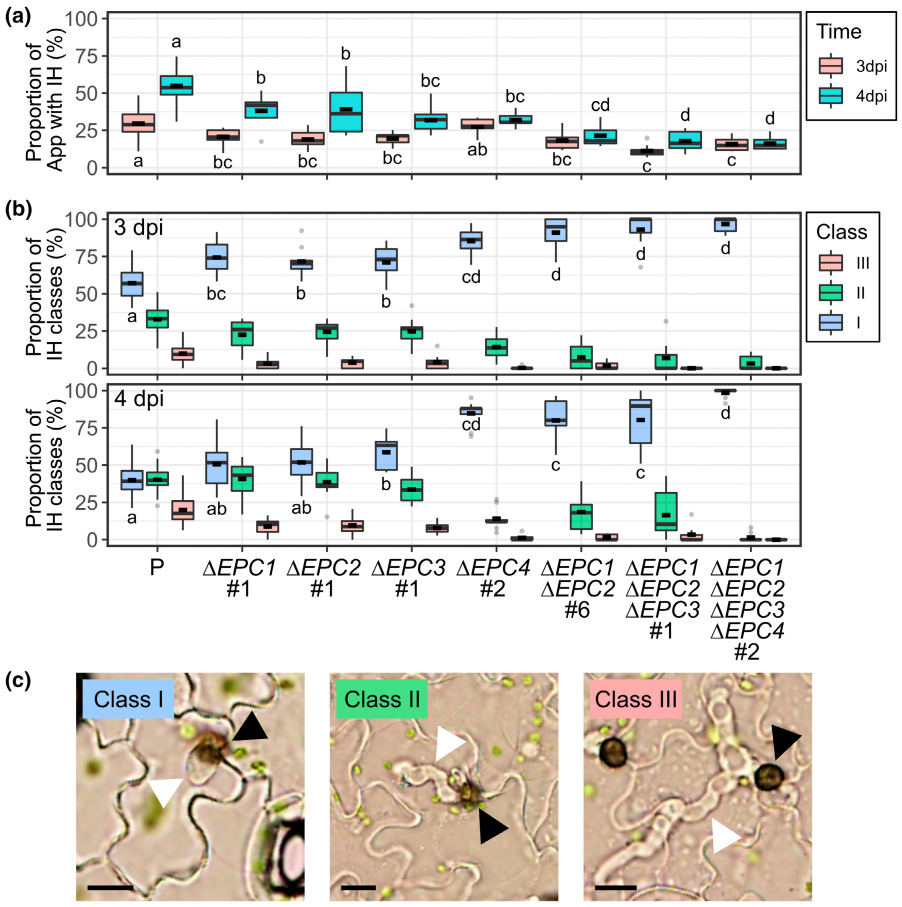

Fig. 4 *EPC* KO mutants are compromised in host penetration and invasive hyphal growth. (a) Boxplot showing the appressoria-mediated invasion (host penetration) ratio of 104-TΔ*lig4* (P) and *EPC* KO mutants. Invasion ratio data were obtained at 3- and 4-d postinoculation (dpi) of cucumber cotyledons. For each mutant, data from nine biological replicates (nine cucumber cotyledons) from three independent experiments (three replicates from each experiment) were obtained. For each replicate, at least 150 appressoria were scored. Thick horizontal bars in black indicate the mean. Center lines show the medians; box limits indicate the 25th and 75th percentiles; whiskers extend to 1.5 times the interquartile range from the 25th and 75th percentiles. For each time point, different letters within the plot indicate significant difference ($P < 0.05$; Tukey HSD test) among the genotypes. (b) Boxplot showing the proportion of invasive hyphae (IH) at different stages of *in planta* growth. Observed IH were classified into three categories based on the length and degree of expansion within the host epidermal cells as shown in (c). Data were taken at 3 and 4 dpi of cucumber cotyledons. Thick horizontal bars in black indicate the mean. Center lines show the medians; box limits indicate the 25th and 75th percentiles; whiskers extend to 1.5 times the interquartile range from the 25th and 75th percentiles. For each time point, different letters within the plot indicate significant difference ($P < 0.05$; Tukey HSD test) among the genotypes. (c) Micrographs showing different stages (class I–III) of invasive growth. Black and white arrowheads indicate appressoria and IH, respectively. Bars, 10 μm. Class I, IH shorter than 10 μm; class II, IH longer than 10 μm and contained within the cell on which penetration occurred; class III, IH longer than 10 μm and extending to more than a single cell.

that collectively contributed to fungal virulence in a host-nonspecific manner (Fig. 6). The Top5 genes were all highly expressed on both hosts, in contrast to *EPC* genes showing host-specific expression patterns (Fig. 6). A contribution of the Top5 genes to virulence was apparent only when all five genes were deleted by multigene KO (Fig. 6); the single-gene KOs yielded no virulence phenotype (Fig. 2b). This indicates either that the Top5 genes are functionally redundant or that each makes too small a contribution to virulence to be detected in our assay condition – or both. Given that candidate effectors often give no virulence phenotype upon single-gene KO (Fig. 2b; Saitoh *et al.*, 2012; Lanver *et al.*, 2017), the multigene KO strategy applied here should be a useful tool to reveal sets of functionally redundant or weak virulence effectors, which can then be subjected to detailed functional characterization. Testing the combination of the Δ*g_04549* mutation and single or multiple KO mutations of the other Top5 genes (*g_13573*, *g_01222*, *g_01264*, and *g_09665*) will allow us to identify the combination of the KO mutations sufficient to give the reduced virulence phenotype.

The host-blind effector, g_04549, has homology to *Magnaporthe oryzae* GAS1 and had roles in successful host invasion (Fig. S18). Consistent with our observations, Xue *et al.* (2002) showed *M. oryzae GAS1* deletion mutants were likewise deficient in host penetration. However, despite containing a signal peptide, GFP tagging analysis showed the GAS1-GFP protein was clearly present in the cytoplasm of appressoria (Xue *et al.*, 2002). Moreover, *GAS1* homologs were highly expressed in *Colletotrichum higginsianum* appressoria formed *in vitro* (Kleemann *et al.*, 2008), suggesting that they are developmentally regulated during

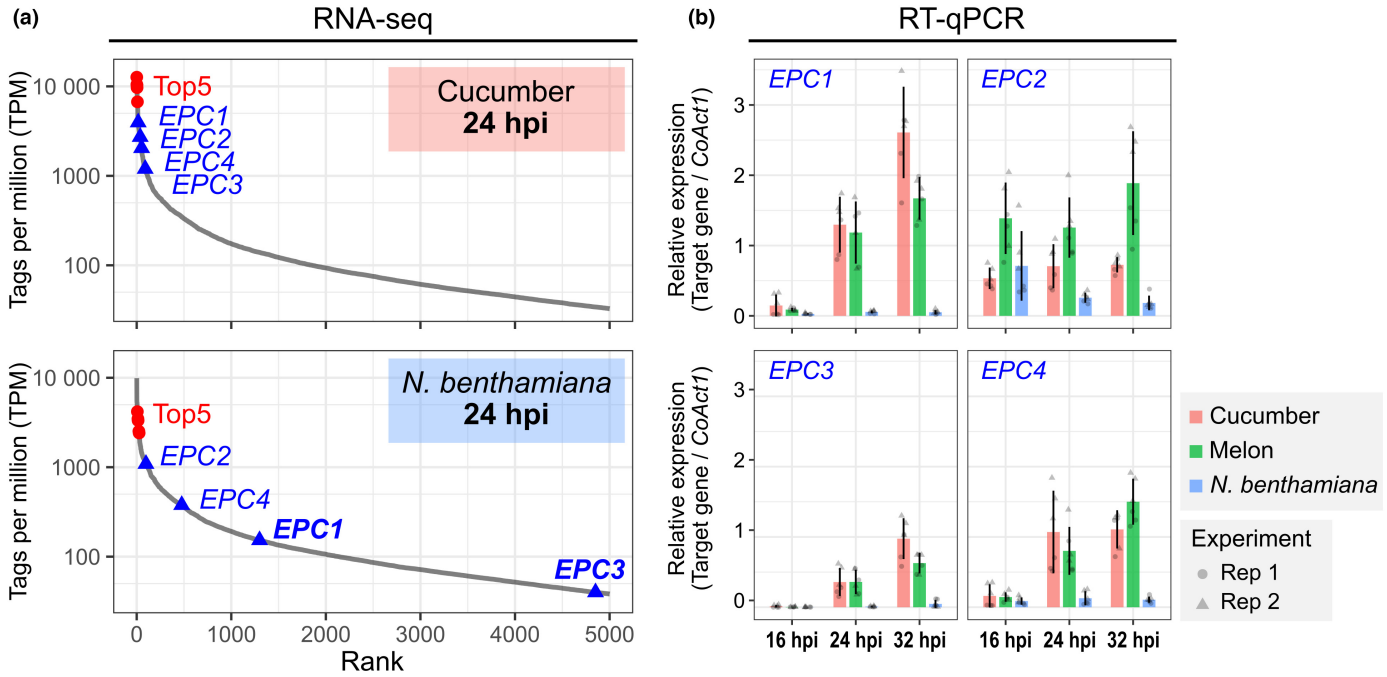

Fig. 5 Gene expression profiles of *EPC*s and the Top5 genes on different host plants. (a) Plot of gene expression values of 5000 genes ranked by gene expression level in RNA-seq data of *Colletotrichum orbiculare* 104-T at 24-h postinoculation (hpi) of cucumber cotyledons (upper panel) and *Nicotiana benthamiana* leaves (lower panel). Genes are arranged in descending order on the *x*-axes. For each gene, expression level in tags per million (TPM) value calculated from the RNA-seq data is plotted on the *y*-axes. The Top5 genes are indicated by red circles, and the four *EPC* genes by blue triangles. Genes in bold are significantly downregulated (FDR < 0.01 in glmTreat test for $|\log_2 FC| > 1$) on *N. benthamiana* compared with on cucumber. (b) Time-course quantification of *EPC* gene expression on cucurbit hosts and *N. benthamiana* by RT-qPCR. Inoculated leaves were sampled at 16, 24, and 32 hpi of cucumber, melon, and *N. benthamiana* and subjected to RT-qPCR with primers for internal control (*C. orbiculare Actin1* gene; 5′-CTCGTTATCGACAATGGTTC-3′ and 5′-GAGTCCTTCTGACCCATACC-3′) and target genes (Supporting Information Table S2). Gene expression levels relative to the internal control are shown. Mean values from six replicates from two independent experiments (three replicates per experiment per condition) are shown as bars. Error bars indicate the 95% confidence interval of the mean.

appressorium morphogenesis and not plant-induced. GAS1 homologs may not be classical secreted effector proteins for host manipulation, but rather play roles in appressorium function, although a recent report has suggested that MoMas3 of *M. oryzae*, a homolog of GAS1, is an apoplastic effector (Gong *et al.*, 2022).

Comparative transcriptome analysis of *C. orbiculare* during cucumber and *N. benthamiana* infection revealed that the overall transcriptional profile is similar in both hosts and that only a small fraction (1.8%) of genes are differentially expressed (Fig. S15). Those DEGs with preferential expression on one of the hosts were significantly enriched in effector candidates, including the host-specific virulence effectors *EPC1* and *EPC3* (Fig. 5). Although we did not detect enrichment of specific functional categories in DEGs with preferential expression on cucumber (Table S7), those with preferential expression on *N. benthamiana* were enriched (11/96, P = 5.4e-03) with carbohydrate-active enzymes (CAZymes; Table S8). Similar host-specific gene expression patterns have been reported in some rust fungi that infect two distantly related alternate hosts during their lifecycle (Duplessis *et al.*, 2021). For example, comparative transcriptome analysis of the heteroecious rust fungus *Melampsora larici-populina* revealed the preferential expression of a small subset of secreted proteins in one of the hosts, while the majority of genes maintained similar expression (Lorrain *et al.*, 2018). Fungal plant pathogens may therefore have strategies that deploy host-specific effectors to establish basic compatibility with specific host families, in addition to conserved general virulence factors that are deployed in a host-blind manner.

Our work revealed that *C. orbiculare* isolates are generally virulent to *N. benthamiana* (Fig. S4a) and infect the Solanaceae species in a similar way as they do on Cucurbitaceae hosts (Figs S1, S5, S6). In addition, an isolate of *Colletotrichum trifolii*, another member of the COSC, showed a similar virulence phenotype on *N. benthamiana* (Fig. S4b). Shen *et al.* (2001) reported that a *Malva* isolate (*Colletotrichum tebeestii* identified by Damm *et al.*, 2013), belonging to the COSC, infects multiple species of the genus *Nicotiana*, including *N. benthamiana*. These observations suggest that multiple members of the COSC can infect *Nicotiana* species, at least under laboratory conditions. Although members of the genus *Nicotiana* have not been described previously as natural hosts for the COSC, *N. benthamiana* may have coexisted with *C. orbiculare* in Australia, where *N. benthamiana* is originated from and *C. orbiculare* has also been isolated from (Shivas *et al.*, 2016), and had some interactions in nature.

The present study has uncovered the contributions of host-specific and host-nonspecific virulence effectors to cucurbit host infection by *C. orbiculare*. *Colletotrichum orbiculare* deploys and depends on general virulence effectors (the Top5 genes) for infection of distantly related hosts of Cucurbitaceae and Solanaceae. In addition to these, four host-specific effectors (EPCs) are required specifically for cucurbit infection. Thus, two classes of effectors,

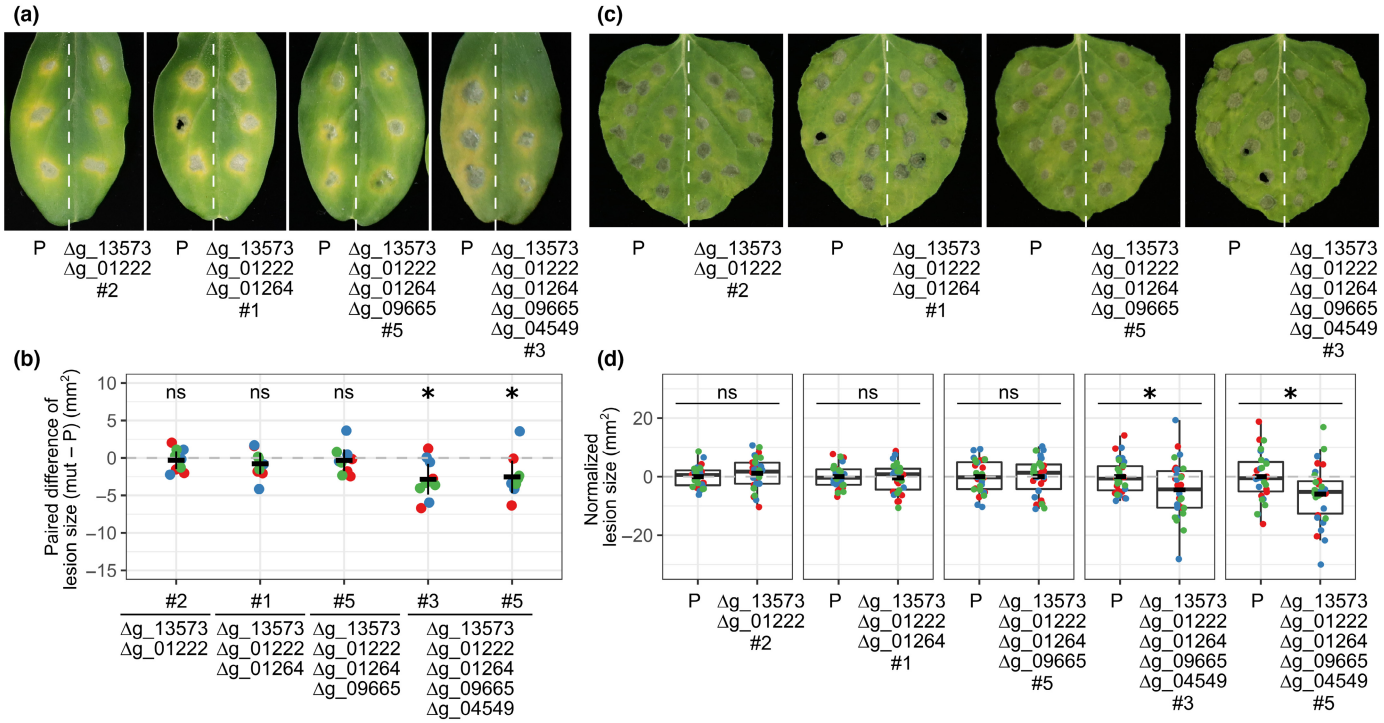

Fig. 6 Multigene KO of the Top5 genes. (a) Lesion formation of the multigene KO mutants on cucumber cotyledons. The left half of the leaf was inoculated with the parental strain for KO (104-TΔ*lig4*, P) and the right half with test strains. Representative pictures taken at 7-d postinoculation (dpi) are shown. (b) Plot showing the virulence effect (paired difference of lesion size) for KO mutants compared with 104-TΔ*lig4* (P). For each mutant, data from nine biological replicates (nine cucumber cotyledons) from three independent experiments (three replicates from each experiment) were obtained and represented as dots. Thick horizontal bars in black indicate paired mean difference of lesion size between respective effector KO mutant (mut) and 104-TΔ*lig4* (P). Error bars indicate the 95% confidence interval of the paired mean difference. Statistical significance in the difference of the mean was tested with the paired *t*-test. (c) Lesion formation of the multigene KO mutants on *Nicotiana benthamiana* leaves. The left half of the leaf was inoculated with the parental strain for KO (104-TΔ*lig4*, P) and the right half with KO mutant strains. Representative pictures taken at 7 dpi are shown. (d) Boxplots showing the lesion size of 104-TΔ*lig4* (P) and KO mutants from paired infection assay as in (c). For each leaf, lesion size data were normalized by mean lesion size of the parental strain. Lesion size data from 8 to 10 drop inoculation sites were collected for each fungal genotype per leaf. Data from 24 to 30 drop inoculation sites from three independent experiments (8–10 drop inoculation sites from one leaf per experiment) were collected. Thick horizontal bars in black indicate the mean. Center lines show the medians; box limits indicate the 25th and 75th percentiles; whiskers extend to 1.5 times the interquartile range from the 25th and 75th percentiles. Statistical significance in the difference of the mean was tested with Welch's *t*-test. *, $P < 0.05$; ns, not significant ($P > 0.05$).

general and host-specific effectors, are involved in host-specific infection by *C. orbiculare*, raising the concept that host species specificity (or basic compatibility for host species) of fungal pathogens depends on host-specific effector deployment that builds on the foundation of general host-blind virulence mechanisms. Although other factors may underlie the successful infection of different hosts, there was a trend that effectors specifically required for infection of cucurbits are preferentially expressed on cucurbit hosts, and those that are required on both hosts have similar expression patterns. How *C. orbiculare* on cucumber specifically expresses a small subset of genes, including *EPC* genes, to establish successful infection remains unclear. Genetic dissection of the host-specific transcriptional control mechanism as well as functional analyses of the EPC effectors will allow us to deepen our understanding of how phytopathogenic fungi have evolved to adapt to their particular host species.

Acknowledgements

We thank the MAFF Genebank for providing *C. orbiculare* isolates MAFF243071, MAFF306870, and MAFF726522 and *C. trifolii* isolate MAFF305383, and Ryutaro Shimada for providing *C. orbiculare* isolate RSCO-09-1-2. We also thank Kyoko Ikeda for technical assistance. This work was supported by Grants-in-Aid for Scientific Research (18H02204 and 21H05032; KAKENHI).

Competing interests

None declared.

Author contributions

YI and YT designed the research. YI, TTPV, SS-O, RZ, KY, TO, JI and YN performed experiments and collected data. YI and YT analyzed data and wrote the manuscript.

ORCID

Yoshihiro Inoue https://orcid.org/0000-0002-0353-1726
Yoshitaka Takano https://orcid.org/0000-0003-1427-1322

Data availability

The data that support the findings of this study are available in the Supporting Information of this article. Nucleotide sequence data reported herein are available in the DNA Data Bank of Japan (DDBJ) Sequence Read Archive under accession no. DRA015571 and in the DDBJ, European Molecular Biology Laboratory, and GenBank databases under accession nos. LC750352, LC750353, LC750354 and LC750355.

References

Altschul SF, Madden TL, Schäffer AA, Zhang J, Zhang Z, Miller W, Lipman DJ. 1997. Gapped Blast and Psi-Blast: a new generation of protein database search programs. *Nucleic Acids Research* **25**: 3389–3402.

Ayukawa Y, Asai S, Gan P, Tsushima A, Ichihashi Y, Shibata A, Komatsu K, Houterman PM, Rep M, Shirasu K *et al.* 2021. A pair of effectors encoded on a conditionally dispensable chromosome of *Fusarium oxysporum* suppress host-specific immunity. *Communications Biology* **4**: 1–12.

Blum M, Chang H-Y, Chuguransky S, Grego T, Kandasaamy S, Mitchell A, Nuka G, Paysan-Lafosse T, Qureshi M, Raj S *et al.* 2021. The InterPro protein families and domains database: 20 years on. *Nucleic Acids Research* **49**: D344–D354.

Cannon PF, Damm U, Johnston PR, Weir BS. 2012. *Colletotrichum* – current status and future directions. *Studies in Mycology* **73**: 181–213.

van Dam P, Fokkens L, Ayukawa Y, van der Gragt M, ter Horst A, Brankovics B, Houterman PM, Arie T, Rep M. 2017. A mobile pathogenicity chromosome in *Fusarium oxysporum* for infection of multiple cucurbit species. *Scientific Reports* **7**: 9042.

Damm U, Cannon PF, Liu F, Barreto RW, Guatimosim E, Crous PW. 2013. The *Colletotrichum orbiculare* species complex: important pathogens of field crops and weeds. *Fungal Diversity* **61**: 29–59.

Dodds PN, Rathjen JP. 2010. Plant immunity: towards an integrated view of plant–pathogen interactions. *Nature Reviews Genetics* **11**: 539–548.

Duplessis S, Lorrain C, Petre B, Figueroa M, Dodds PN, Aime MC. 2021. Host adaptation and virulence in heteroecious rust fungi. *Annual Review of Phytopathology* **59**: 403–422.

Eddy SR. 2011. Accelerated profile HMM searches. *PLoS Computational Biology* **7**: e1002195.

Gan P, Ikeda K, Irieda H, Narusaka M, O'Connell RJ, Narusaka Y, Takano Y, Kubo Y, Shirasu K. 2013. Comparative genomic and transcriptomic analyses reveal the hemibiotrophic stage shift of *Colletotrichum* fungi. *New Phytologist* **197**: 1236–1249.

Gan P, Tsushima A, Narusaka M, Narusaka Y, Takano Y, Kubo Y, Shirasu K. 2019. Genome sequence resources for four phytopathogenic fungi from the *Colletotrichum orbiculare* species complex. *Molecular Plant–Microbe Interactions* **32**: 1088–1090.

Gawehns F, Houterman PM, Ichou FA, Michielse CB, Hijdra M, Cornelissen BJC, Rep M, Takken FLW. 2014. The *Fusarium oxysporum* effector Six6 contributes to virulence and suppresses I-2-mediated cell death. *Molecular Plant–Microbe Interactions* **27**: 336–348.

Gong Z, Ning N, Li Z, Xie X, Wilson RA, Liu W. 2022. Two *Magnaporthe* appressoria-specific (MAS) proteins, MoMas3 and MoMas5, are required for suppressing host innate immunity and promoting biotrophic growth in rice cells. *Molecular Plant Pathology* **23**: 1290–1302.

Grabherr MG, Haas BJ, Yassour M, Levin JZ, Thompson DA, Amit I, Adiconis X, Fan L, Raychowdhury R, Zeng Q *et al.* 2011. Trinity: reconstructing a full-length transcriptome without a genome from RNA-Seq data. *Nature Biotechnology* **29**: 644–652.

Gu Z, Eils R, Schlesner M. 2016. Complex heatmaps reveal patterns and correlations in multidimensional genomic data. *Bioinformatics* **32**: 2847–2849.

Haas BJ, Delcher AL, Mount SM, Wortman JR, Smith RK, Hannick LI, Maiti R, Ronning CM, Rusch DB, Town CD *et al.* 2003. Improving the *Arabidopsis* genome annotation using maximal transcript alignment assemblies. *Nucleic Acids Research* **31**: 5654–5666.

Haas BJ, Salzberg SL, Zhu W, Pertea M, Allen JE, Orvis J, White O, Buell CR, Wortman JR. 2008. Automated eukaryotic gene structure annotation using EvidenceModeler and the program to assemble spliced alignments. *Genome Biology* **9**: R7.

Heath MC. 1981. A generalized concept of host-parasite specificity. *Phytopathology* **71**: 1121.

Hoff KJ, Lange S, Lomsadze A, Borodovsky M, Stanke M. 2016. Braker1: unsupervised RNA-Seq-based genome annotation with GeneMark-ET and Augustus. *Bioinformatics* **32**: 767–769.

Huang W, Hong S, Tang G, Lu Y, Wang C. 2019. Unveiling the function and regulation control of the DUF3129 family proteins in fungal infection of hosts. *Philosophical Transactions of the Royal Society of London. Series B: Biological Sciences* **374**: 20180321.

Huerta-Cepas J, Szklarczyk D, Forslund K, Cook H, Heller D, Walter MC, Rattei T, Mende DR, Sunagawa S, Kuhn M *et al.* 2016. eggNOG 4.5: a hierarchical orthology framework with improved functional annotations for eukaryotic, prokaryotic and viral sequences. *Nucleic Acids Research* **44**: D286–D293.

Irieda H, Inoue Y, Mori M, Yamada K, Oshikawa Y, Saitoh H, Uemura A, Terauchi R, Kitakura S, Kosaka A *et al.* 2019. Conserved fungal effector suppresses PAMP-triggered immunity by targeting plant immune kinases. *Proceedings of the National Academy of Sciences, USA* **116**: 496–505.

Irieda H, Maeda H, Akiyama K, Hagiwara A, Saitoh H, Uemura A, Terauchi R, Takano Y. 2014. *Colletotrichum orbiculare* secretes virulence effectors to a biotrophic interface at the primary hyphal neck via exocytosis coupled with SEC22-mediated traffic. *Plant Cell* **26**: 2265–2281.

Isozumi N, Inoue Y, Imamura T, Mori M, Takano Y, Ohki S. 2019. Ca^{2+}-dependent interaction between calmodulin and CoDN3, an effector of *Colletotrichum orbiculare*. *Biochemical and Biophysical Research Communications* **514**: 803–808.

Jayawardena R. 2016. Notes on currently accepted species of *Colletotrichum*. *Mycosphere* **7**: 1192–1260.

Käll L, Krogh A, Sonnhammer ELL. 2004. A combined transmembrane topology and signal peptide prediction method. *Journal of Molecular Biology* **338**: 1027–1036.

Kanja C, Hammond-Kosack KE. 2020. Proteinaceous effector discovery and characterization in filamentous plant pathogens. *Molecular Plant Pathology* **21**: 1353–1376.

Kim D, Paggi JM, Park C, Bennett C, Salzberg SL. 2019. Graph-based genome alignment and genotyping with Hisat2 and Hisat-genotype. *Nature Biotechnology* **37**: 907–915.

Kleemann J, Rincon-Rivera LJ, Takahara H, Neumann U, van Themaat EVL, van der Does HC, Hacquard S, Stüber K, Will I, Schmalenbach W *et al.* 2012. Sequential delivery of host-induced virulence effectors by appressoria and intracellular hyphae of the phytopathogen *Colletotrichum higginsianum*. *PLoS Pathogens* **8**: e1002643.

Kleemann J, Takahara H, Stüber K, O'Connell R. 2008. Identification of soluble secreted proteins from appressoria of *Colletotrichum higginsianum* by analysis of expressed sequence tags. *Microbiology* **154**: 1204–1217.

Kubo Y, Takano Y. 2013. Dynamics of infection-related morphogenesis and pathogenesis in *Colletotrichum orbiculare*. *Journal of General Plant Pathology* **79**: 233–242.

Lanver D, Tollot M, Schweizer G, Lo Presti L, Reissmann S, Ma L-S, Schuster M, Tanaka S, Liang L, Ludwig N *et al.* 2017. *Ustilago maydis* effectors and their impact on virulence. *Nature Reviews Microbiology* **15**: 409–421.

Li B, Dewey CN. 2011. Rsem: accurate transcript quantification from RNA-Seq data with or without a reference genome. *BMC Bioinformatics* **12**: 323.

Li J, Fokkens L, van Dam P, Rep M. 2020. Related mobile pathogenicity chromosomes in *Fusarium oxysporum* determine host range on cucurbits. *Molecular Plant Pathology* **21**: 761–776.

Liao Y, Smyth GK, Shi W. 2019. The R package Rsubread is easier, faster, cheaper and better for alignment and quantification of RNA sequencing reads. *Nucleic Acids Research* **47**: e47.

Liu B, Wasilwa LA, Morelock TE, O'Neill NR, Correll JC. 2007. Comparison of *Colletotrichum orbiculare* and several allied *Colletotrichum* spp. for mtDNA RFLPs, intron RFLP and sequence variation, vegetative compatibility, and host specificity. *Phytopathology* **97**: 1305–1314.

Lomsadze A, Burns PD, Borodovsky M. 2014. Integration of mapped RNA-Seq reads into automatic training of eukaryotic gene finding algorithm. *Nucleic Acids Research* **42**: e119.

Lorrain C, Marchal C, Hacquard S, Delaruelle C, Pétrowski J, Petre B, Hecker A, Frey P, Duplessis S. 2018. The rust fungus *Melampsora larici-populina* expresses a conserved genetic program and distinct sets of secreted protein genes during infection of its two host plants, larch and poplar. *Molecular Plant–Microbe Interactions* **31**: 695–706.

Matsuo H, Ishiga Y, Kubo Y, Yoshioka Y. 2022. *Colletotrichum orbiculare* strains distributed in Japan: race identification and evaluation of virulence to cucurbits. *Breeding Science* **72**: 306–315.

McCarthy DJ, Chen Y, Smyth GK. 2012. Differential expression analysis of multifactor RNA-Seq experiments with respect to biological variation. *Nucleic Acids Research* **40**: 4288–4297.

McCarthy DJ, Smyth GK. 2009. Testing significance relative to a fold-change threshold is a TREAT. *Bioinformatics* **25**: 765–771.

Mistry J, Chuguransky S, Williams L, Qureshi M, Salazar GA, Sonnhammer ELL, Tosatto SCE, Paladin L, Raj S, Richardson LJ *et al.* 2021. Pfam: the protein families database in 2021. *Nucleic Acids Research* **49**: D412–D419.

Münch S, Lingner U, Floss DS, Ludwig N, Sauer N, Deising HB. 2008. The hemibiotrophic lifestyle of *Colletotrichum* species. *Journal of Plant Physiology* **165**: 41–51.

Nielsen H. 2017. Predicting secretory proteins with SignalP. In: Kihara D, ed. *Methods in molecular biology. Protein function prediction: methods and protocols*. New York, NY, USA: Springer, 59–73.

Niks RE, Marcel TC. 2009. Nonhost and basal resistance: how to explain specificity? *New Phytologist* **182**: 817–828.

Niu X, Zhao X, Ling K-S, Levi A, Sun Y, Fan M. 2016. The *FonSIX6* gene acts as an avirulence effector in the *Fusarium oxysporum* f. sp. *niveum* – watermelon pathosystem. *Scientific Reports* **6**: 28146.

O'Connell RJ, Thon MR, Hacquard S, Amyotte SG, Kleemann J, Torres MF, Damm U, Buiate EA, Epstein L, Alkan N *et al.* 2012. Lifestyle transitions in plant pathogenic *Colletotrichum* fungi deciphered by genome and transcriptome analyses. *Nature Genetics* **44**: 1060–1065.

Panstruga R, Moscou MJ. 2020. What is the molecular basis of nonhost resistance? *Molecular Plant–Microbe Interactions* **33**: 1253–1264.

Perfect SE, Hughes HB, O'Connell RJ, Green JR. 1999. *Colletotrichum*: a model genus for studies on pathology and fungal–plant interactions. *Fungal Genetics and Biology* **27**: 186–198.

de Queiroz CB, Correia HLN, Menicucci RP, Vidigal PMP, de Queiroz MV. 2017. Draft genome sequences of two isolates of *Colletotrichum lindemuthianum*, the causal agent of anthracnose in common beans. *Genome Announcements* **5**: e00214-17.

Rawlings ND, Barrett AJ, Thomas PD, Huang X, Bateman A, Finn RD. 2018. The Merops database of proteolytic enzymes, their substrates and inhibitors in 2017 and a comparison with peptidases in the Panther database. *Nucleic Acids Research* **46**: D624–D632.

Ristaino JB, Anderson PK, Bebber DP, Brauman KA, Cunniffe NJ, Fedoroff NV, Finegold C, Garrett KA, Gilligan CA, Jones CM *et al.* 2021. The persistent threat of emerging plant disease pandemics to global food security. *Proceedings of the National Academy of Sciences, USA* **118**: e2022239118.

Robinson MD, McCarthy DJ, Smyth GK. 2010. edgeR: a Bioconductor package for differential expression analysis of digital gene expression data. *Bioinformatics* **26**: 139–140.

Robinson MD, Oshlack A. 2010. A scaling normalization method for differential expression analysis of RNA-seq data. *Genome Biology* **11**: R25.

Saitoh H, Fujisawa S, Mitsuoka C, Ito A, Hirabuchi A, Ikeda K, Irieda H, Yoshino K, Yoshida K, Matsumura H *et al.* 2012. Large-scale gene disruption in *Magnaporthe oryzae* identifies MC69, a secreted protein required for infection by monocot and dicot fungal pathogens. *PLoS Pathogens* **8**: e1002711.

Schulze-Lefert P, Panstruga R. 2011. A molecular evolutionary concept connecting nonhost resistance, pathogen host range, and pathogen speciation. *Trends in Plant Science* **16**: 117–125.

Shen S, Goodwin PH, Hsiang T. 2001. Infection of *Nicotiana* species by the anthracnose fungus, *Colletotrichum orbiculare*. *European Journal of Plant Pathology* **107**: 767–773.

Shivas RG, Tan YP, Edwards J, Dinh Q, Maxwell A, Andjic V, Liberato JR, Anderson C, Beasley DR, Bransgrove K *et al.* 2016. *Colletotrichum* species in Australia. *Australasian Plant Pathology* **45**: 447–464.

Stanke M, Keller O, Gunduz I, Hayes A, Waack S, Morgenstern B. 2006. Augustus: *ab initio* prediction of alternative transcripts. *Nucleic Acids Research* **34**: W435–W439.

Sweigard J, Chumley F, Carroll A, Farrall L, Valent B. 1997. A series of vectors for fungal transformation. *Fungal Genetics Reports* **44**: 52–53.

Takano Y, Komeda K, Kojima K, Okuno T. 2001. Proper regulation of cyclic AMP-dependent protein kinase is required for growth, conidiation, and appressorium function in the anthracnose fungus *Colletotrichum lagenarium*. *Molecular Plant–Microbe Interactions* **14**: 1149–1157.

Takano Y, Takayanagi N, Hori H, Ikeuchi Y, Suzuki T, Kimura A, Okuno T. 2006. A gene involved in modifying transfer RNA is required for fungal pathogenicity and stress tolerance of *Colletotrichum lagenarium*. *Molecular Microbiology* **60**: 81–92.

Thordal-Christensen H, Birch PRJ, Spanu PD, Panstruga R. 2018. Why did filamentous plant pathogens evolve the potential to secrete hundreds of effectors to enable disease? *Molecular Plant Pathology* **19**: 781–785.

Toruño TY, Stergiopoulos I, Coaker G. 2016. Plant-pathogen effectors: cellular probes interfering with plant defenses in spatial and temporal manners. *Annual Review of Phytopathology* **54**: 419–441.

Valette N, Renou J, Boutilliat A, Fernández-González AJ, Gautier V, Silar P, Guyeux C, Charr J-C, Cuenot S, Rose C *et al.* 2021. OSIP1 is a self-assembling DUF3129 protein required to protect fungal cells from toxins and stressors. *Environmental Microbiology* **23**: 1594–1607.

Xue C, Park G, Choi W, Zheng L, Dean RA, Xu J-R. 2002. Two novel fungal virulence genes specifically expressed in appressoria of the rice blast fungus. *Plant Cell* **14**: 2107–2119.

Yamada K, Yamamoto T, Uwasa K, Osakabe K, Takano Y. 2023. The establishment of multiple knockout mutants of *Colletotrichum orbiculare* by CRISPR-Cas9 and Cre-*loxP* systems. *Fungal Genetics and Biology* **165**: 103777.

Yin Y, Mao X, Yang J, Chen X, Mao F, Xu Y. 2012. dbCAN: a web resource for automated carbohydrate-active enzyme annotation. *Nucleic Acids Research* **40**: W445–W451.

Yoshino K, Irieda H, Sugimoto F, Yoshioka H, Okuno T, Takano Y. 2012. Cell death of *Nicotiana benthamiana* is induced by secreted protein NIS1 of *Colletotrichum orbiculare* and is suppressed by a homologue of CgDN3. *Molecular Plant–Microbe Interactions* **25**: 625–636.

Zhang R, Isozumi N, Mori M, Okuta R, Singkaravanit-Ogawa S, Imamura T, Gan P, Shirasu K, Ohki S, Takano Y. 2021. Fungal effector SIB1 of *Colletotrichum orbiculare* has unique structural features and can suppress plant immunity in *Nicotiana benthamiana*. *Journal of Biological Chemistry* **297**: 101370.

Supporting Information

Additional Supporting Information may be found online in the Supporting Information section at the end of the article.

Dataset S1 Amico acid sequences of 13 287 protein-coding genes of *Colletotrichum orbiculare* 104-T predicted in this study.

Fig. S1 Cytological observation of cucumber infection by *Colletotrichum orbiculare* 104-T.

Fig. S2 Differentially expressed genes between *in vitro* and *in planta* conditions.

Fig. S3 Schematic representation of the experimental design for quantification of virulence effect on cucumber.

Fig. S4 Virulence of isolates from the *Colletotrichum orbiculare* species complex on *Nicotiana benthamiana*.

Fig. S5 Lesion development by *Colletotrichum orbiculare* on cucurbit hosts and *Nicotiana benthamiana*.

Fig. S6 Cytological observation of *Nicotiana benthamiana* infection by *Colletotrichum orbiculare* 104-T.

Fig. S7 Amino acid sequence of EPC1 and comparisons with its homologs.

Fig. S8 Amino acid sequence of EPC2 and phylogenetic relationships of its homologs.

Fig. S9 Alignment of amino acid sequences of EPC4 homologs.

Fig. S10 Amino acid sequence of EPC3 and phylogenetic relationships and virulence contribution of its homologs.

Fig. S11 Knockout (KO) vectors for generation of *EPC* multigene KO mutants and maps of genomic regions around the target genes.

Fig. S12 Quantification of fungal biomass by qPCR.

Fig. S13 Appressorium formation ratio of *EPC* knockout strains.

Fig. S14 Measurement of appressorial penetration of inert cellophane membranes by *EPC* quadruple knockout mutants.

Fig. S15 Differentially expressed genes of *Colletotrichum orbiculare* during infection of two distantly related host species, cucumber and *Nicotiana benthamiana*.

Fig. S16 Knockout (KO) vectors for generation of the Top5 multigene KO mutants and maps of genomic regions around the target genes.

Fig. S17 Genetic complementation of the Top5 quintuple knockout mutant.

Fig. S18 Quantification of host penetration and invasive hyphal growth of the Top5 quintuple knockout mutants.

Fig. S19 Appressoria formation of the Top5 quintuple knockout mutants on different hosts.

Fig. S20 Hyphal growth of the Top5 quintuple knockout mutants on PDA medium.

Fig. S21 Amino acid sequence of g_04549.

Fig. S22 Alignment of amino acid sequences of g_09965 homologs from *Colletotrichum* species.

Fig. S23 Alignment of amino acid sequences of g_13573 homologs from *Colletotrichum* species.

Fig. S24 Amino acid sequence and phylogenetic relationships of g_01264 homologs.

Fig. S25 Amino acid sequence and phylogenetic relationships of g_01222 homologs.

Table S1 *Colletotrichum orbiculare* isolates used in this study.

Table S2 Primers used in this study.

Table S3 *Colletotrichum orbiculare* strains used in this study.

Table S4 Summary of RNA-seq reads and mapping statistics.

Table S5 Plasmids used in this study.

Table S6 List of *in planta*-induced core secreted protein genes of *Colletotrichum orbiculare*.

Table S7 Significantly upregulated *Colletotrichum orbiculare* genes on cucumber compared with on *Nicotiana benthamiana* at 24 hpi.

Table S8 Significantly upregulated *Colletotrichum orbiculare* genes on *Nicotiana benthamiana* compared with on cucumber at 24 hpi.

Please note: Wiley is not responsible for the content or functionality of any Supporting Information supplied by the authors. Any queries (other than missing material) should be directed to the *New Phytologist* Central Office.